Blind CFO Estimators for OFDM/OQAM Systems With Null Subcarriers

Tilde Fusco and Mario Tanda
Dipartimento di Ingegneria Elettronica e delle Telecomunicazioni,
Università di Napoli Federico II,
via Claudio 21, I-80125 Napoli, Italy.
E-mail: {tilfusco, tanda}@unina.it

***Abstract*— This paper deals with the problem of blind carrier-frequency offset (CFO) estimation in OFDM systems based on offset quadrature amplitude modulation (OFDM/OQAM) with null subcarriers. Specifically, by assuming that the number of subcarriers is sufficiently large, the received signal is modeled as a complex Gaussian random vector (CGRV). Since the OFDM/OQAM signal results to be a noncircular (NC) process, by exploiting the generalized probability density function for NC-CGRVs, the unconditional maximum likelihood (ML) algorithm for CFO estimation in non dispersive channel is proposed. Moreover, a modified version of the unconditional ML CFO estimator is considered. The performance of the derived algorithms, assessed via computer simulation, is compared with that of recently proposed estimators exploiting the second-order cyclostationarity and with the Gaussian Cramér-Rao bound.**

***Index Terms*— Blind estimation, carrier-frequency offset, null subcarries, OFDM/OQAM systems.**

I. INTRODUCTION

Orthogonal frequency-division multiplexing (OFDM) modulation is well known for its robustness to multipath channels. This is mainly due to the insertion of a guard interval (or cyclic prefix) that efficiently combat the intersymbol interference and the intercarrier interference in dispersive channels. However, the insertion of a guard interval is pure redundancy, and then it decreases the spectral efficiency. Therefore, it is interesting to study alternative OFDM modulation schemes, which can provide the same robustness without requiring a guard interval, offering a better spectral efficiency. For this purpose, recently, a new efficient OFDM scheme based on offset quadrature amplitude modulation (OFDM/OQAM) has been developed (see [1]- [5] and references therein). Moreover, OFDM/OQAM systems with null (or virtual) subcarriers have also been investigated by the IEEE 802.22 working group [6].

However, like all the other multicarrier modulation schemes, OFDM/OQAM systems are in general more sensitive to frequency synchronization errors than single-carrier systems, [7] and [8]. In particular, a carrier-frequency offset (CFO) induces an amplitude reduction of the transmitted signal and provokes intersymbol and intercarrier interference [9]. Therefore, accurate CFO synchronization schemes must be designed for these systems.

In [10] a blind CFO estimation algorithm has been derived by exploiting the conjugate second-order cyclostationarity of the received OFDM signal in the case of noncircular transmissions. In [5] this method, designed for standard OFDM systems, has been extended and analyzed in the context of OFDM/OQAM transmissions. However, the derived estimator assures a satisfactory performance only when a large number of OFDM symbols is considered. The second-order conjugate cyclostationarity has been also exploited in [11] while in [12] a blind joint CFO and symbol timing estimator based on the unconjugate cyclostationarity property of the OFDM/OQAM signal has been derived.

This paper, by considering the study addressed in [13], proposes blind CFO estimation algorithms for OFDM/OQAM systems with virtual subcarriers. Specifically, by assuming that the number of subcarriers is sufficiently large, the received signal is modeled as a complex Gaussian random vector (CGRV). Moreover, it is shown that the OFDM/OQAM signal results to be a noncircular (NC) (or improper [14]) process (i.e., its conjugate correlation function is different from zero [5]). Therefore, by exploiting the generalized probability density function (pdf) for NC-CGRVs reported in [15] and under the hypothesis of a non dispersive channel, the unconditional maximum likelihood (ML) algorithm for CFO estimation is derived. Moreover, a modified version of the unconditional ML CFO estimator is considered. The performance of the derived algorithms, assessed via computer simulation, is compared with that of the estimators proposed in [12] and in [5], exploiting the second-order cyclostationarity, and with the Gaussian Cramér-Rao bound.

The organization of this paper is as follows. In Section II we describe the considered system model. Section III deals with the ML CFO estimation algorithm. The GCRB is derived in Section IV and numerical results are presented and discussed in Section V. Finally, conclusions are drawn in Section VI.

Notation: $j \triangleq \sqrt{-1}$, superscript $(\cdot)^*$ denotes the complex conjugation, $\Re[\cdot]$ real part, $\Im[\cdot]$ imaginary part, $|\cdot|$ absolute value and $\arg[\cdot]$ the argument of a complex number in $[0, 2\pi)$. Moreover, $(\cdot)^T$ indicates transpose,

This work was supported in part by the Italian Ministry of University (MIUR) project S.Co.P.E.

$(\cdot)^H$ Hermitian, $(\cdot)^{-1}$ the inverse of a matrix, $\boldsymbol{I}_n$ ($\boldsymbol{O}_n$) is the $n \times n$ identity (null) matrix, $\mathbf{1}_n$ is an n-dimensional column vector of all ones and $[\boldsymbol{A}]_{(m,l)}$ is the (m,l)th entry of the matrix $\boldsymbol{A}$. In addition, $\mathrm{diag}\{\cdot\}$ is a diagonal matrix, $\mathrm{Tr}\{\cdot\}$ the trace operator, $\det\{\cdot\}$ the determinant of a matrix while $E[\cdot]$ stands for the statistical expectation and $\delta(k)$ is the Kronecker delta. Finally, lower (upper) case boldface symbols denote column vectors (matrices).

II. Signal Model

Let us consider the OFDM/OQAM system with N subcarriers, of which N_v subcarriers remain unmodulated and carry no information while $N_u = N - N_v$ are modulated by data subcarriers. The discrete-time received signal in AWGN channel and in the presence of a CFO ν and a carrier phase offset ϕ can be written as

$$r(k) = s(k)e^{j[2\pi\nu k+\phi]} + n(k) \tag{1}$$

where $s(k)$ is the transmitted OFDM/OQAM signal and $n(k)$ denotes the zero-mean circular complex white Gaussian noise statistically independent of $s(k)$. The signal $s(k)$ is given by

$$s(k)=\sum_{p=-\infty}^{\infty}\left[x^R_{p,(k-pN)}+j\,x^I_{p,(k-pN)}\right] \tag{2}$$

where $x^R_{p,m}$ and $x^I_{p,m}$ are given by

$$x^R_{p,m} \triangleq \sqrt{\frac{N}{2N_u}}\sum_{l=-N_u/2}^{N_u/2-1} a^R_{p,l}e^{j\frac{2\pi}{N}lm}g(m) \tag{3}$$

$$x^I_{p,m} \triangleq \sqrt{\frac{N}{2N_u}}\sum_{l=-N_u/2}^{N_u/2-1} a^I_{p,l}e^{j\frac{2\pi}{N}lm}g\left(m-\frac{N}{2}\right) \tag{4}$$

In (3) and (4) the sequences $a^R_{p,l}$ and $a^I_{p,l}$ denote the real and imaginary parts of the complex data symbols transmitted on the lth subcarrier during the pth OFDM/OQAM symbol and $g(k)$ denotes the real transmitted pulse-shaping filter. It is assumed that

- AS1) The data symbols $\{a^R_{p,l}\}_{p=-\infty}^{\infty}$ and $\{a^I_{p,l}\}_{p=-\infty}^{\infty}$, $\forall l \in \{-N_u/2,\ldots,N_u/2-1\}$, belonging to a PAM constellation, are statistically independent and identically distributed random variables with zero mean and $E[|a^R_{p,l}|^2] = E[|a^I_{p,l}|^2] = \sigma_a^2$.
- AS2) The number of useful subcarriers N_u is sufficiently large so that the OFDM/OQAM signal $s(k)$ can be modeled as a complex Gaussian process.

Let us observe that from the assumptions (AS1) and (AS2) we can easily derive the following results:

Result 1: The unconjugate correlation function of the transmitted OFDM/OQAM signal $s(k)$ at time k and lag l is equal to

$$C_s(k;l) \triangleq E\left[s^*(k)s(k+l)\right]$$

$$=\frac{N\sigma_a^2}{2N_u}\sum_{m=-N_u/2}^{N_u/2-1} e^{j\frac{2\pi}{N}ml}$$

$$\times\sum_{p=-\infty}^{\infty} g\left(k-\frac{pN}{2}\right)g\left(k+l-\frac{pN}{2}\right)$$

$$=\frac{\sigma_a^2}{N_u}\sum_{m=-N_u/2}^{N_u/2-1} e^{j\frac{2\pi}{N}ml}$$

$$\times\sum_{q=0}^{N/2-1} e^{j\frac{4\pi}{N}q(k+l)}\int_{-1/2}^{1/2}G(\nu)G^*\left(\nu-\frac{2q}{N}\right)e^{-j2\pi\nu l}\mathrm{d}\nu \tag{5}$$

where

$$G(\mu) = \sum_{k=-\infty}^{\infty} g(k)e^{-j2\pi k\mu} \tag{6}$$

is the discrete-time Fourier transform (DFT) of the real unit-energy pulse-shaping filter $g(k)$.

Result 2: The relation function (or the conjugate correlation function) of the transmitted signal $s(k)$ is given by

$$R_s(k;l) \triangleq E\left[s(k)s(k+l)\right]$$

$$=\frac{N\sigma_a^2}{2N_u}\sum_{m=-N_u/2}^{N_u/2-1} e^{j\frac{2\pi}{N}m(2k+l)}$$

$$\times\sum_{p=-\infty}^{\infty}(-1)^p g\left(k-\frac{pN}{2}\right)g\left(k+l-\frac{pN}{2}\right) \tag{7}$$

$$=\frac{\sigma_a^2}{2N_u}\sum_{m=-N_u/2}^{N_u/2-1} e^{j\frac{2\pi}{N}m(2k+l)}\sum_{q=0}^{N-1}\left[1-(-1)^q\right]$$

$$\times e^{j\frac{2\pi}{N}q(k+l)}\int_{-1/2}^{1/2}G(\nu)G^*\left(\nu-\frac{q}{N}\right)e^{-j2\pi\nu l}\mathrm{d}\nu.$$

From result 1 we can observe that the unconjugate correlation function is $N/2$-periodic in k. Therefore, the transmitted OFDM/OQAM signal results to be unconjugate second-order cyclostationary with period $N/2$. On the other hand, from result 2 we can note that the conjugate correlation function results to be conjugate second-order cyclostationary with period N.

In the absence of virtual subcarriers (that is for $N = N_u$) and in the presence of a pulse-shaping filter satisfying the orthogonality condition [4]

$$\sum_{p=-\infty}^{\infty} g\left(k-\frac{pN}{2}\right)g\left(k+\beta N-\frac{pN}{2}\right)=\frac{2}{N}\delta(\beta)$$

$$\forall\beta\in\mathbb{Z}$$

the unconjugate correlation function of the transmitted OFDM/OQAM signal $s(k)$ at time k and lag l is equal to (see [13])

$$\begin{aligned} C_s(k;l) &= \frac{N\sigma_a^2}{2}\delta(l-\beta\,N) \\ &\times \sum_{p=-\infty}^{\infty} g\left(k-\frac{pN}{2}\right) g\left(k+l-\frac{pN}{2}\right) \\ &= \sigma_a^2\delta(l)\,. \end{aligned} \tag{8}$$

Moreover, the conjugate correlation function results to be

$$\begin{aligned} R_s(k;l) &= \frac{N\sigma_a^2}{2}\delta(2k+l-\beta\,N) \\ &\times \sum_{p=-\infty}^{\infty} (-1)^p g\left(k-\frac{pN}{2}\right) g\left(k+l-\frac{pN}{2}\right)\,. \end{aligned} \tag{9}$$

From (8) we can deduce that the absence of virtual subcarriers can destroy the unconjugate cyclostationarity of the OFDM/OQAM signal. In fact, in this case the OFDM/OQAM signal is stationary with respect to its unconjugate correlation function but cyclostationary with respect to its conjugate correlation function.

III. ML CFO Estimator

In this section the ML CFO estimator for OFDM/OQAM systems is derived by maximizing the log-likelihood function (LLF) for the vector of unknown parameters $\boldsymbol{\lambda} \triangleq [\nu,\phi]^T$. Precisely, let us consider the observation vector $\boldsymbol{r}$ of total length $W=\eta N$

$$\boldsymbol{r} = \boldsymbol{\Psi}(\boldsymbol{\lambda})\boldsymbol{s} + \boldsymbol{n} \tag{10}$$

where

$$\boldsymbol{\Psi}(\boldsymbol{\lambda}) \triangleq \mathrm{diag}\left\{e^{j\phi},\ldots,e^{j[2\pi\nu(\eta N-1)+\phi]}\right\}$$

is the $W\times W$ diagonal matrix parameterized by the vector of unknown parameters $\boldsymbol{\lambda}$. Moreover,

$$\boldsymbol{s} \triangleq [s(0),\ldots,s\,(W-1)]^T$$

is the transmitted OFDM/OQAM vector, while $\boldsymbol{n}$ denotes the noise vector modeled as a zero-mean circular CGRV with covariance matrix $E[\boldsymbol{n}\boldsymbol{n}^H]=\sigma_n^2\boldsymbol{I}_W$.

The observations vector $\boldsymbol{r} \triangleq [r(0),\ldots,r(W-1)]^T$ results to be a zero-mean NC-CGRV and, then, is characterized by the joint pdf [15]

$$\begin{aligned} f(\boldsymbol{r},\boldsymbol{r}^*;\boldsymbol{\lambda}) &= \frac{1}{\pi^W\sqrt{\det\{\bar{\boldsymbol{C}}\}}} \\ &\times \exp\left\langle -\frac{1}{2}\left[\boldsymbol{r}^H\boldsymbol{r}^T\right]\bar{\boldsymbol{C}}^{-1}\begin{bmatrix}\boldsymbol{r}\\ \boldsymbol{r}^*\end{bmatrix}\right\rangle \end{aligned} \tag{11}$$

where

$$\bar{\boldsymbol{C}} \triangleq E\left\{\begin{bmatrix}\boldsymbol{r}\\ \boldsymbol{r}^*\end{bmatrix}\left[\boldsymbol{r}^H,\boldsymbol{r}^T\right]\right\} = \begin{bmatrix}\boldsymbol{C}_{\boldsymbol{r}} & \boldsymbol{R}_{\boldsymbol{r}}\\ \boldsymbol{R}_{\boldsymbol{r}}^H & \boldsymbol{C}_{\boldsymbol{r}}^*\end{bmatrix} \tag{12}$$

with

$$\boldsymbol{C}_{\boldsymbol{r}} \triangleq E[\boldsymbol{r}\boldsymbol{r}^H] = \boldsymbol{\Psi}(\boldsymbol{\lambda})\left[\underbrace{E[\boldsymbol{s}\boldsymbol{s}^H]}_{\boldsymbol{C}_{\boldsymbol{s}}}+\sigma_n^2\boldsymbol{I}_W\right]\boldsymbol{\Psi}^*(\boldsymbol{\lambda}) \tag{13}$$

while

$$\boldsymbol{R}_{\boldsymbol{r}} \triangleq E[\boldsymbol{r}\boldsymbol{r}^T] = \boldsymbol{\Psi}(\boldsymbol{\lambda})\underbrace{E[\boldsymbol{s}\boldsymbol{s}^T]}_{\boldsymbol{R}_{\boldsymbol{s}}}\boldsymbol{\Psi}(\boldsymbol{\lambda}) \tag{14}$$

is the so-called relation matrix.

By using the equalities $\boldsymbol{R}_{\boldsymbol{s}}^H=\boldsymbol{R}_{\boldsymbol{s}}^*$ and $\boldsymbol{C}_{\boldsymbol{s}}^T=\boldsymbol{C}_{\boldsymbol{s}}^*$ and the properties of inversion of block matrices we have

$$\begin{aligned} &\bar{\boldsymbol{C}}^{-1} \\ &= \begin{bmatrix} \boldsymbol{Q}_{\boldsymbol{s}}^{-1} & -(\boldsymbol{C}_{\boldsymbol{s}}+\sigma_n^2\boldsymbol{I})^{-1}\boldsymbol{R}_{\boldsymbol{s}}\boldsymbol{Q}_{\boldsymbol{s}}^{-*} \\ -(\boldsymbol{C}_{\boldsymbol{s}}^*+\sigma_n^2\boldsymbol{I})^{-1}\boldsymbol{R}_{\boldsymbol{s}}^*\boldsymbol{Q}_{\boldsymbol{s}}^{-1} & \boldsymbol{Q}_{\boldsymbol{s}}^{-*} \end{bmatrix} \end{aligned} \tag{15}$$

where

$$\boldsymbol{Q}_{\boldsymbol{s}} = \boldsymbol{C}_{\boldsymbol{s}}+\sigma_n^2\boldsymbol{I}_W-\boldsymbol{R}_{\boldsymbol{s}}\left[\boldsymbol{C}_{\boldsymbol{s}}^*+\sigma_n^2\boldsymbol{I}_W\right]^{-1}\boldsymbol{R}_{\boldsymbol{s}}^*$$

is the Schur complement of the matrix $\boldsymbol{C}_{\boldsymbol{s}}^*+\sigma_n^2\boldsymbol{I}_W$.

Substituting (15) in (11) and dropping the constant

$$\frac{1}{\pi^W\sqrt{\det\{\bar{\boldsymbol{C}}\}}}$$

independent of the parameters to estimate, we obtain that the LLF for the vector of parameters of interest can be written as

$$\begin{aligned} \Lambda(\boldsymbol{\lambda}) &= \log\left[f(\boldsymbol{r},\boldsymbol{r}^*;\boldsymbol{\lambda})\right] \\ &= \Re\left\{-\boldsymbol{r}^H\boldsymbol{\Psi}(\boldsymbol{\lambda})\boldsymbol{Q}_{\boldsymbol{s}}^{-1}\boldsymbol{\Psi}^*(\boldsymbol{\lambda})\boldsymbol{r}\right. \\ &\quad +\boldsymbol{r}^T\boldsymbol{\Psi}^*(\boldsymbol{\lambda})\left[\boldsymbol{C}_{\boldsymbol{s}}^*+\sigma_n^2\boldsymbol{I}_W\right]^{-1} \\ &\quad \left.\times\boldsymbol{R}_{\boldsymbol{s}}^*\boldsymbol{Q}_{\boldsymbol{s}}^{-1}\boldsymbol{\Psi}^*(\boldsymbol{\lambda})\boldsymbol{r}\right\}\,. \end{aligned} \tag{16}$$

The joint ML estimator is obtained by searching the value of the vector $\boldsymbol{\lambda}$ that maximizes the LLF. To proceed we keep the parameter ν fixed and let ϕ vary. In these conditions the function $\Lambda(\boldsymbol{\lambda})$ in (16) achieves a maximum for

$$\begin{aligned} \hat{\phi}_{ML}(\nu) = &\frac{1}{2}\arg\left\{\boldsymbol{r}^T\boldsymbol{\Upsilon}^*(\nu)\left[\boldsymbol{C}_{\boldsymbol{s}}^*+\sigma_n^2\boldsymbol{I}_W\right]^{-1}\right. \\ &\left.\times\boldsymbol{R}_{\boldsymbol{s}}^*\boldsymbol{Q}_{\boldsymbol{s}}^{-1}\boldsymbol{\Upsilon}^*(\nu)\boldsymbol{r}\right\}, \end{aligned} \tag{17}$$

where $\boldsymbol{\Upsilon}(\nu) \triangleq \mathrm{diag}\left\{1,\ldots,e^{j2\pi\nu(\eta N-1)}\right\}$. Then, accounting for (16) and (17), the ML CFO estimator is given by

$$\begin{aligned} \hat{\nu}_{ML} = \arg\max_{\tilde{\nu}} &\left\langle -\Re\left\{\boldsymbol{r}^H\boldsymbol{\Upsilon}(\tilde{\nu})\boldsymbol{Q}_{\boldsymbol{s}}^{-1}\boldsymbol{\Upsilon}^*(\tilde{\nu})\boldsymbol{r}\right\}\right. \\ &\left.+\left|\boldsymbol{r}^T\boldsymbol{\Upsilon}^*(\tilde{\nu})\left[\boldsymbol{C}_{\boldsymbol{s}}^*+\sigma_n^2\boldsymbol{I}_W\right]^{-1}\boldsymbol{R}_{\boldsymbol{s}}^*\boldsymbol{Q}_{\boldsymbol{s}}^{-1}\boldsymbol{\Upsilon}^*(\tilde{\nu})\boldsymbol{r}\right|\right\rangle \end{aligned} \tag{18}$$

where $\tilde{\nu}$ is a trial value for CFO.

Putting the relation matrix $\boldsymbol{R_s} = \boldsymbol{O}_W$ in (16), the expression of the LLF becomes

$$\Lambda(\nu) = -\Re\left\{\boldsymbol{r}^H \boldsymbol{\Upsilon}(\nu)\left[\boldsymbol{C_s} + \sigma_n^2 \boldsymbol{I}_W\right]^{-1} \boldsymbol{\Upsilon}^*(\nu)\boldsymbol{r}\right\}. \tag{19}$$

Note that in this case the LLF does not depend on the carrier phase ϕ and, moreover, the expression of the corresponding CFO estimator exploiting uniquely the unconjugate correlation matrix $\boldsymbol{C_s}$ (labeled as unconjugate ML estimator) is given by

$$\hat{\nu}_{UML} = \arg\max_{\tilde{\nu}} \left\langle -\Re\left\{\boldsymbol{r}^H \boldsymbol{\Upsilon}(\tilde{\nu})\left[\boldsymbol{C_s} + \sigma_n^2 \boldsymbol{I}_W\right]^{-1} \boldsymbol{\Upsilon}^*(\tilde{\nu})\boldsymbol{r}\right\}\right\rangle. \tag{20}$$

In Fig. 1 we report the behavior, in a single run, of CFO metrics in (18) and (20) as a function of ν, for an OFDM/OQAM system with $N = 16$ subcarriers, $N_u = 12$ active subcarriers, $\eta = 32$ OFDM/OQAM symbols and for SNR $\triangleq \sigma_a^2/\sigma_n^2 = 20$ dB. As shown in the figure the metric in (18) exploiting both the unconjugate and the conjugate cyclostationarity of the OFDM/OQAM signal presents a sharp peak at the actual value of the CFO. Instead, the UML metric exploiting only the unconjugate cyclostationarity of the OFDM/OQAM signal appears much more flat.

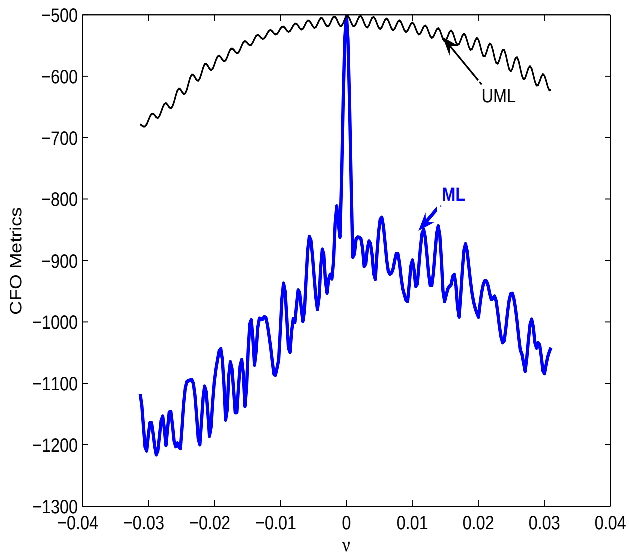

Figure 1. Behavior, in a single run, of CFO metrics as a function of ν for an OFDM/OQAM system with $N = 16$, $N_u = 12$, $\eta = 32$ and SNR $= 20$ dB.

IV. Gaussian Cramér-Rao bound

In this section we evaluate the CRB on CFO and carrier phase estimation for OFDM/OQAM systems. Note that since a Gaussianity assumption is imposed on the data vector and due to the noncircularity of the OFDM/OQAM signal, the derived CRB is the Gaussian [16] (or stochastic [17]) CRB for NC complex distributions. Therefore, as shown in [17] and [16], the (i, m)th entry of the Fisher information matrix (FIM) for the vector of the parameters of interest $\boldsymbol{\lambda}$, is given by

$$[\boldsymbol{F}]_{(i,m)} = \tfrac{1}{2}\mathrm{Tr}\left[\frac{\partial \bar{\boldsymbol{C}}}{\partial\lambda(i)}\bar{\boldsymbol{C}}^{-1}\frac{\partial \bar{\boldsymbol{C}}}{\partial\lambda(m)}\bar{\boldsymbol{C}}^{-1}\right] \quad \forall i, m \in \{0, 1\} \tag{21}$$

where the matrix $\bar{\boldsymbol{C}}$ is defined in (12). Substituting (12) into (21) and after algebraic manipulations we obtain the 2×2 FIM

$$\boldsymbol{F} = \begin{bmatrix} 8\pi^2 \mathrm{Tr}\{\boldsymbol{D}_\nu \boldsymbol{\Delta}_\nu\} & 4\pi \mathrm{Tr}\{\boldsymbol{D}_\nu \boldsymbol{\Delta}_\phi\} \\ 4\pi \mathrm{Tr}\{\boldsymbol{D}_\nu \boldsymbol{\Delta}_\phi\} & 2\mathrm{Tr}\{\boldsymbol{\Delta}_\phi\} \end{bmatrix} \tag{22}$$

where the matrix $\boldsymbol{\Delta}_{\lambda(i)}$ $\forall i \in \{0, 1\}$ is given by

$$\boldsymbol{\Delta}_{\lambda(i)} = \Re\{[\boldsymbol{C_s} + \sigma_n^2 \boldsymbol{I}_W]\boldsymbol{D}_{\lambda(i)}\boldsymbol{Q_s}^{-1} + \boldsymbol{R_s}\boldsymbol{D}_{\lambda(i)}[\boldsymbol{C}_{\boldsymbol{s}}^* + \sigma_n^2 \boldsymbol{I}_W]^{-1}\boldsymbol{R}_{\boldsymbol{s}}^*\boldsymbol{Q_s}^{-1} - \boldsymbol{D}_{\lambda(i)}\}$$

with $\boldsymbol{D}_{\lambda(0)} \triangleq \mathrm{diag}\{0, \ldots, W-1\}$ and $\boldsymbol{D}_{\lambda(1)} \triangleq \boldsymbol{I}_W$.

The CRB for ν and ϕ is given by the corresponding inverse FIM diagonal element, that is

$$\mathrm{CRB}_\nu = \frac{1}{8\pi^2}\left\{\mathrm{Tr}[\boldsymbol{D}_\nu\boldsymbol{\Delta}_\nu] - \mathrm{Tr}[\boldsymbol{D}_\nu\boldsymbol{\Delta}_\phi]^2\,\mathrm{Tr}[\boldsymbol{\Delta}_\phi]^{-1}\right\}^{-1} \tag{23}$$

and

$$\mathrm{CRB}_\phi = \frac{1}{2}\left\{\mathrm{Tr}[\boldsymbol{\Delta}_\phi] - \mathrm{Tr}[\boldsymbol{D}_\nu\boldsymbol{\Delta}_\phi]^2\,\mathrm{Tr}[\boldsymbol{D}_\nu\boldsymbol{\Delta}_\nu]^{-1}\right\}^{-1}. \tag{24}$$

The right hand side of (23) and (24) depends, through unmanageable relations, on the number of observed symbols η, on the number of active subcarriers N_u, on the SNR value, and on the pulse-shaping filter $g(k)$. Therefore, in the following a numerical example is carried out to show this dependence. Precisely, Fig.s 2 and 3 report the behavior of bounds (23) and (24) normalized to $1/\eta^3$ and $1/\eta$, respectively, as a function of the number of OFDM/OQAM symbols η in the case of a square-root raised cosine pulse $g(k)$ with a rolloff parameter ρ. The numerical results have been obtained for an SNR value fixed at SNR $= 20$ dB and for different values of the rolloff parameter ρ. By investigating these plots we can observe that the CRB_ν decreases at the rate $1/\eta^3$ and, moreover, the bound is lower for higher values of the rolloff parameter. Moreover, as shown in Fig. 3 and according to [16], the CRB_ϕ is inversely proportional to η.

V. Numerical Results and Comparison

In this section the performance of ML and UML CFO estimators reported in (18) and (20), respectively, is assessed via computer simulations and compared with that of Bölcskei's algorithm derived in [12] and that of the CFO estimator proposed by Ciblat and Serpedin in [5] and labeled in the following as CS estimator. The actual values of the CFO and of the carrier phase have been fixed at $\nu = 1/(4W)$ and $\phi = \pi/8$, respectively, while

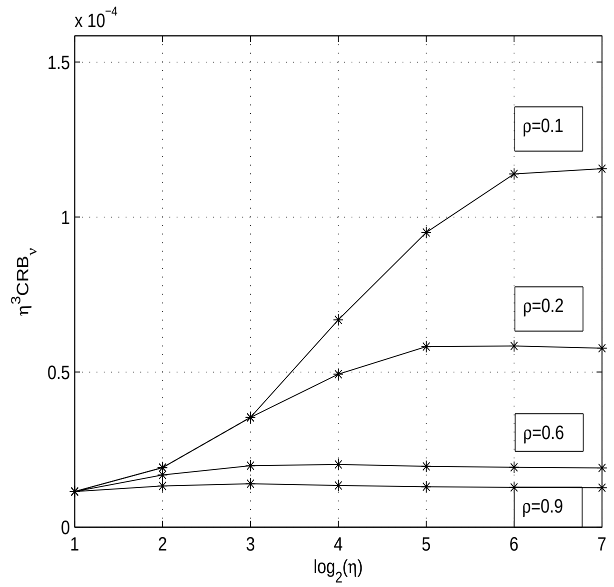

Figure 2. Behavior of $\eta^3\mathrm{CRB}_\nu$ versus $\log_2(\eta)$ for $\rho\in\{0.1, 0.2, 0.6, 0.9\}$, SNR=20 dB, $N = 16$ and $N_u = 12$.

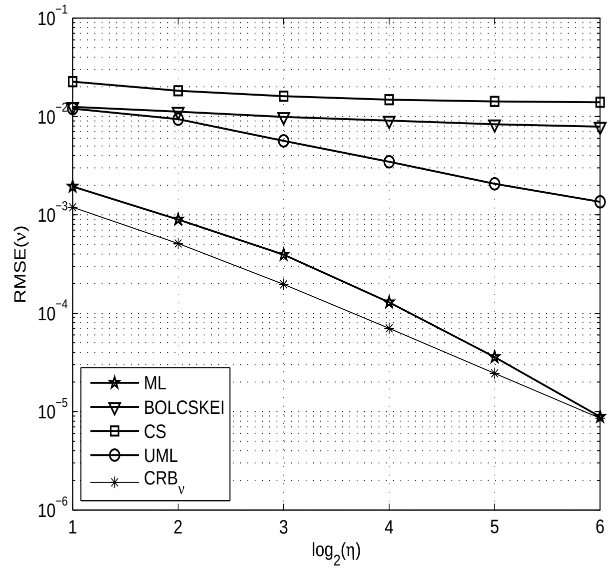

Figure 4. Performance of the considered CFO estimators in AWGN channel as a function of the number of observed OFDM/OQAM symbols η, for $N = 16$, $N_u = 12$ and $\mathrm{SNR} = 20$ dB.

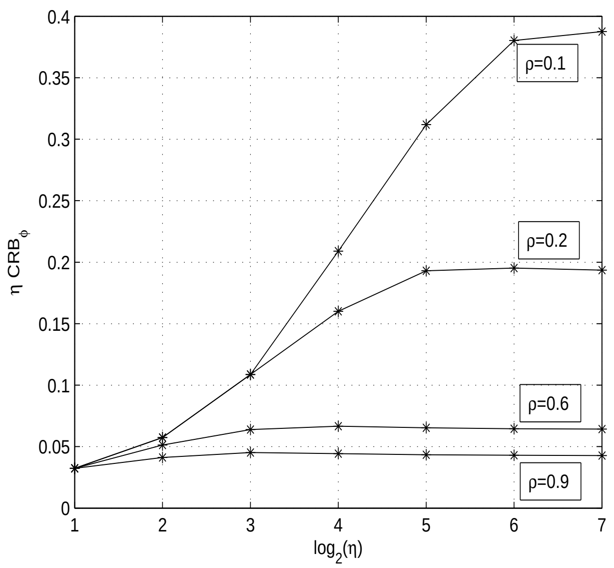

Figure 3. Behavior of $\eta\mathrm{CRB}_\phi$ versus $\log_2(\eta)$ for $\rho\in\{0.1, 0.2, 0.6, 0.9\}$, SNR=20 dB, $N = 16$ and $N_u = 12$.

10^3 trials have been used to obtain the performance plot. Moreover, in all the simulation results we consider an OFDM/OQAM system employing a pulse-shaping filter $g(k)$ given by a square-root raised cosine with a rolloff parameter $\rho = 0.6$.

A. AWGN Channel

In Fig.4 we compare the root mean-square error (RMSE) of ML, UML, CS and Bölcskei's algorithms as a function of the number of observed symbols η for an OFDM/OQAM system with $N = 16$ total subcarriers, $N_u = 12$ active subcarriers and in the presence of an AWGN channel with $\mathrm{SNR} = 20$dB. Moreover, the GCRB obtained from (23) is also shown as a comparison. From Fig. 4 we can see that the ML CFO estimator reveals the best performance among all considered estimators and assures an RMSE very close to the corresponding GCRB while the UML CFO estimator presents an higher RMSE. This is principally due to the much more flat behavior of the UML CFO metric with respect to the ML CFO cost function (see Fig. 1).

Fig. 5 presents the performance of the considered algorithms as a function of SNR for an OFDM/OQAM system with $N = 16$ subcarriers and an observation window of length $W = 32N$. The results show that the CFO ML estimator achieves the GCRB at SNR values higher than 20 dB. Moreover, the CS estimator, demanding much more large observation intervals, reveals a severe performance degradation in the whole range of the considered SNR values.

B. Multipath Channel

The performance of the considered estimators has also been assessed in the presence of an unknown multipath channel. In each experiment the multipath channel $h(l)$ has been modeled to consist of N_m+1=4 independent Rayleigh-fading taps with an exponentially decaying power delay profile. Specifically, $E[|h(l)|^2] = Ce^{-l/4}$, $l \in \{0, \ldots, N_m\}$, where C is a constant such that $\sum_{l=0}^{N_m} E[|h(l)|^2] = 1$. Moreover, the channel is fixed in the observation window but independent from one run to another.

Fig. 6 displays the RMSE of ML, UML, CS and Bölcskei's algorithms as a function of the number of observed OFDM/OQAM symbols. As we can see, all the considered algorithms present a significant performance

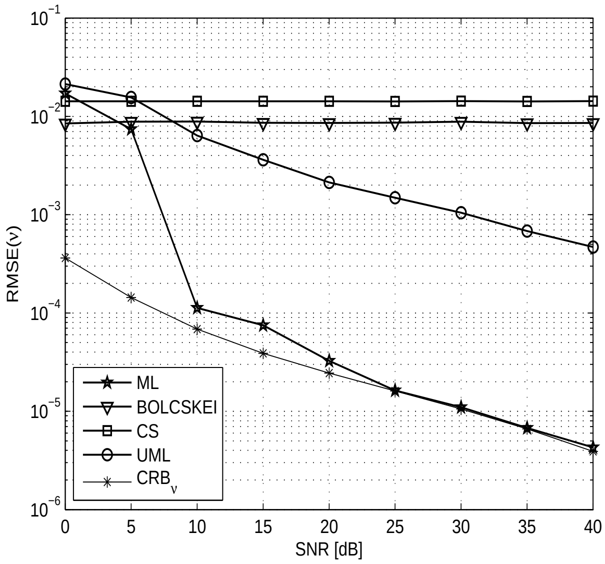

Figure 5. Performance of the considered CFO estimators in AWGN channel as a function of SNR for a number of observed OFDM/OQAM symbols $\eta = 32$ for $N = 16$ and $N_u = 12$.

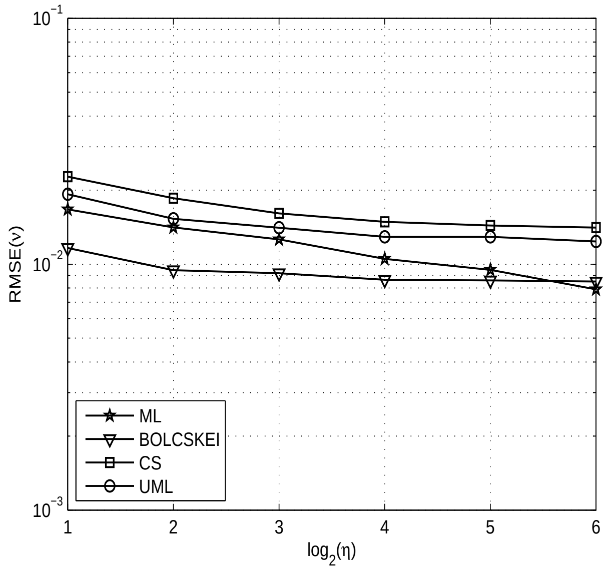

Figure 6. Performance of the considered CFO estimators in multipath channel as a function of the number of observed OFDM/OQAM symbols η for $N = 16$, $N_u = 12$ and $\mathrm{SNR} = 20$ dB.

degradation with respect to that in AWGN channel due to the model mismatch. In particular, the ML CFO estimator can outperform the Bölcskei's estimator only for a relatively large number of symbols. Finally, the results reported in Fig.7 show the RMSE of the considered CFO estimators as a function of SNR for a sample size fixed at $W = 2^9$. We can note that in the presence of a dispersive channel the UML CFO estimator can provide the most accurate estimates for high SNR values.

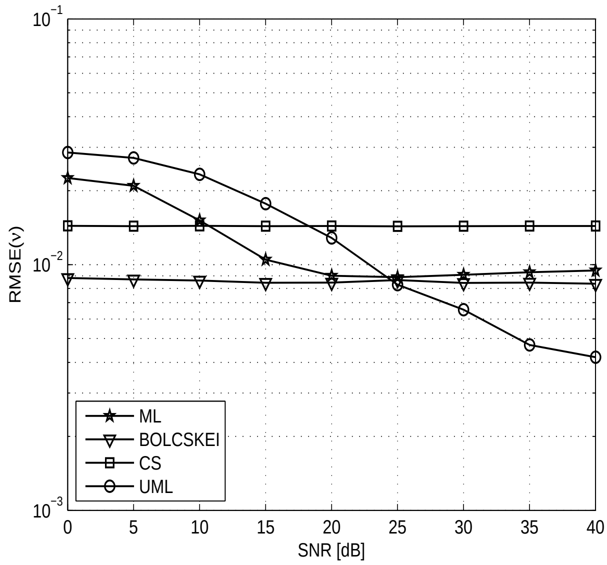

Figure 7. Performance of the considered CFO estimators in multipath channel as a function of SNR for $N = 16$, $N_u = 12$ and $\eta = 32$.

VI. CONCLUSIONS

In this paper the problem of blind CFO estimation in OFDM/OQAM systems in the presence of virtual subcarriers has been considered. In particular, under the hypothesis that the number of useful subcarriers is sufficiently large, the transmitted OFDM/OQAM signal has been modeled as an NC-CGRV. Exploiting the generalized expression of the pdf for NC-CGRVs, the joint ML estimator for the parameters of interest has been derived. Moreover, a modified version of the ML CFO estimator is considered. The performance of the derived estimators has been compared with that of the CS estimator derived in [5] and that of the Bölcskei's algorithm proposed in [12]. As illustrated by computer simulations, in AWGN the considered estimators outperform those proposed in [5] and [12] while in multipath channel the proposed estimators can assure a satisfactory performance if a sufficiently large number of observed symbols or high SNR values are considered.

REFERENCES

[1] H. Bölcskei, P. Duhamel and R. Hleiss,"A subspace-based approach to blind channel identification in pulse shaping OFDM/OQAM systems," *IEEE Trans. Signal Processing*, vol. 49, pp. 1594-1598, July 2001.

[2] D. Lacroix, N. Goudard and M. Alard,"OFDM with guard interval versus OFDM/offsetQAM for high data rate UMTS downlink transmission," Proc. of *VTC 2001 Fall*, vol. 4, October 2001, pp. 2682-2686.

[3] P. Siohan, C. Siclet and N. Lacaille, "Analysis and design of OFDM/OQAM systems based on filterbank theory," *IEEE Trans. Signal Processing*, vol. 50, pp. 1170-1183, May 2002.

[4] H. Bölcskei, P. Duhamel and R. Hleiss,"Orthogonalization of OFDM/OQAM pulse shaping filters using the discrete Zak transform," *Signal Processing*, vol. 83, pp. 1379-1391, July 2003.

[5] P. Ciblat and E. Serpedin, "A fine blind frequency offset estimator for OFDM/OQAM systems," *IEEE Trans. Signal*

Processing, vol. 52, pp. 291-296, January 2004.
[6] D. Birru, V. Gaddam, C. Cordeiro, K. Challapali, M. Bellec, P. Pirat, L. Escobar, and D. Callonec, "A Cognitive PHY/MAC Proposal for IEEE 802.22 Systems-Part 1: The Cognitive PHY," IEEE 802.22 document no. 22-05-0103-r0, November 2005, http://www.ieee802.org/22/.
[7] L. Wei and C. Schlegel, "Synchronization requirements for multi-user OFDM on satellite mobile and two-path Rayleigh fading channels," *IEEE Trans. Commun.*, vol. 43, pp. 887-895, Feb./Mar./Apr. 1995.
[8] T. Pollet and M. Moeneclaey, "Synchronizability of OFDM signals," Proc. of *GLOBECOM 1995*, November 1995, pp. 2054-2058.
[9] P. K. Remvik, N. Holte, A. Vahlin,"Fading and carrier frequency offset robustness for different pulse shaping filters in OFDM," Proc. of *VTC 1998*, May 1998, pp. 777-781.
[10] P. Ciblat and L. Vandendorpe, "Blind carrier frequency offset estimation for noncircular constellation-based transmissions," *IEEE Trans. Signal Processing*, vol. 51, pp. 1378-1389, May 2003.
[11] G. Lin, L. Lundheim, and N. Holte, "New methods for blind fine estimation of carrier frequency offset in OFDM/OQAM systems," Proc. of *SPAWC06*, July 2006, Cannes, France.
[12] H. Bölcskei, "Blind estimation of symbol timing and carrier frequency offset in wireless OFDM systems," *IEEE Trans. Commun.*, vol. 49, pp. 988-999, June 2001.
[13] T. Fusco and M. Tanda, "Blind frequency-offset estimation for OFDM/OQAM systems," *IEEE Trans. Signal Processing*, vol. 55, pp. 1828-1838, May 2007.
[14] F.D. Neeser and J.L. Massey, "Proper complex random processes with applications to information theory," *IEEE Trans. Inform. Theory*, vol. 39, pp. 1293-1302, July 1993.
[15] B. Picinbono, "Second-order complex random vectors and normal distributions," *IEEE Trans. Signal Processing*, vol. 44, pp. 2637-2640, October 1996.
[16] P. Ciblat, M. Ghogho, P. Forster and P. Larzabal, "Harmonic retrieval in the presence of non-circular Gaussian multiplicative noise: performance bounds," *Signal Processing*, vol. 85, pp. 737-749, April 2005.
[17] J.P. Delmas and H. Abeida, "Stochastic Cramér-Rao bound for noncircular signals with application to DOA estimation," *IEEE Trans. Signal Processing*, vol. 52, pp. 3192-3199, November 2004.

Tilde Fusco was born in Napoli, Italy, on March 22, 1977. She received the Dr. Eng. degree (summa cum laude) in electronic engineering from the Second University of Napoli, Napoli, Italy, in 2002 and the Ph.D. degree in electronic and telecommunication engineering from the University of Napoli Federico II, Napoli, Italy, in 2006. In 2006, she was awarded a postdoctoral fellowship at the University of Napoli Federico II, where she is currently pursuing her research activity. Her current research and study interests lie in the area of statistical signal processing, with emphasis on parameter estimation problems in the context of orthogonal-frequency-division multiplexing (OFDM) communications.

Mario Tanda was born in Aversa, Italy, on July 15, 1963. He received the Dr. Eng. degree (summa cum laude) in electronic engineering and the Ph.D. degree in electronic and computer engineering from the University of Napoli Federico II, Napoli, Italy, in 1987 and 1992, respectively. Since 1995, he has been an Appointed Professor of signal theory at the University of Napoli Federico II. Moreover, he has been an Appointed Professor of electrical communications (from 1996 until 1997) and telecommunication systems (from 1997) at the Second University of Napoli, Napoli, Italy. He is currently a Full Professor of Telecommunications at the University of Napoli Federico II. His research activity is in the area of signal detection and estimation, multicarrier, and multiple- access communication systems.